Combined Treatment with Peptide-Conjugated Phosphorodiamidate Morpholino Oligomer-PPMO and AAV-U7 Rescues the Severe DMD Phenotype in Mice

Anne Forand, Antoine Muchir, Nathalie Mougenot, Caroline Sévoz-Couche, Cécile Peccate, Mégane Lemaitre, Charlotte Izabelle, Matthew Wood, Stéphanie Lorain, France Pietri-Rouxel

Molecular Therapy
Methods & Clinical Development
Original Article

Combined Treatment with Peptide-Conjugated Phosphorodiamidate Morpholino Oligomer-PPMO and AAV-U7 Rescues the Severe DMD Phenotype in Mice

Anne Forand,[1] Antoine Muchir,[1] Nathalie Mougenot,[2] Caroline Sevoz-Couche,[3] Cécile Peccate,[1] Mégane Lemaitre,[2] Charlotte Izabelle,[1] Matthew Wood,[4,5] Stéphanie Lorain,[1,6] and France Piétri-Rouxel[1,6]

[1]Centre de Recherche en Myologie, Sorbonne Université, UMRS974, INSERM, Institut de Myologie-Faculté de Médecine de la Pitié Salpêtrière, 105 boulevard de l'Hôpital, 75013 Paris, France; [2]Sorbonne Université, UPMC Paris 06, INSERM UMS28, Phénotypage du petit animal, Faculté de Médecine Pierre et Marie Curie, 91 boulevard de l'Hôpital, 75013 Paris, France; [3]Sorbonne Université, UPMC Univ Paris 06, INSERM UMRS1158, Neurophysiologie Respiratoire Expérimentale et Clinique, Faculté de Médecine Pierre et Marie Curie, 91 boulevard de l'Hôpital, 75013 Paris, France; [4]Department of Paediatrics, University of Oxford, Oxford OX3 9DU, United Kingdom; [5]MDUK Oxford Neuromuscular Centre, University of Oxford, Oxford OX3 9DU, United Kingdom

Duchenne muscular dystrophy (DMD) is a devastating neuromuscular disease caused by an absence of the dystrophin protein, which is essential for muscle fiber integrity. Among the developed therapeutic strategies for DMD, the exon-skipping approach corrects the frameshift and partially restores dystrophin expression. It could be achieved through the use of antisense sequences, such as peptide-conjugated phosphorodiamidate morpholino oligomer (PPMO) or the small nuclear RNA-U7 carried by an adeno-associated virus (AAV) vector. AAV-based gene therapy approaches have potential for use in DMD treatment but are subject to a major limitation: loss of the AAV genome, necessitating readministration of the vector, which is not currently possible, due to the immunogenicity of the capsid. The PPMO approach requires repeated administrations and results in only weak cardiac dystrophin expression. Here, we evaluated a combination of PPMO- and AAV-based therapy in a mouse model of severe DMD. Striking benefits of this combined therapy were observed in striated muscles, with marked improvements in heart and diaphragm structure and function, with unrivalled extent of survival, opening novel therapeutic perspectives for patients.

INTRODUCTION

Duchenne muscular dystrophy (DMD) is an X-linked severe neuromuscular disorder caused by mutations of the *DMD* gene,[1] leading to the absence of dystrophin, a protein essential for muscle fiber integrity during the contraction process.[2] DMD affects 1 in 5,000 male births and is characterized by progressive degeneration of striated muscles, causing a loss of ambulation, cardiomyopathy, respiratory failure, and ultimately death.[3,4] Several therapeutic approaches for DMD are currently being investigated.[5] The most recently developed treatment is gene therapy based on CRISPR-Cas9 editing, for which long-term efficacy has been demonstrated.[6,7] However, this approach introduces unintended changes to the genome and transcripts,[7] and therapeutic interventions require improvement, as shown by a study of gene editing via homology-directed repair in the dog model of DMD.[8]

The antisense oligonucleotide (AO)-mediated, exon-skipping strategy aims to force pre-mRNA splicing to remove the mutated exon, restoring the in-frame sequence of the transcript and leading to the expression of a shorter but functional dystrophin.[9] The AOs originally used were degraded by endonucleases and/or exonucleases and therefore, had a limited therapeutic effect.[10] In the phosphorodiamidate morpholino backbone (PMO), a third generation of AOs, a nonribose-based modification, prevents degradation by nucleases, but the nonionic structure of these compounds reduces their nuclear uptake.[11] Furthermore, limitations to the use of PMOs in DMD treatment were highlighted in several animal-based studies reporting poor cellular uptake, rapid clearance from the bloodstream, an inability to cross the blood-brain barrier,[12] and weak effects on the diaphragm and heart.[13] In the latest generation of AOs, short cell-penetrating peptides have been conjugated to PMO (PPMOs) to increase their ability to penetrate into cells.[14,15] PPMOs, like all of the other AOs produced to date, have the enormous advantage of not being immunogenic, but they must be administered regularly to sustain

Received 20 February 2020; accepted 12 March 2020;
https://doi.org/10.1016/j.omtm.2020.03.011.

[6]These authors contributed equally to this work.

Correspondence: France Piétri-Rouxel, PhD, Centre de Recherche en Myologie, Sorbonne Université, UMRS974, INSERM, Institut de Myologie-Faculté de Médecine de la Pitié Salpêtrière, 105 boulevard de l'Hôpital, 75013 Paris, France.
E-mail: france.pietri-rouxel@upmc.fr
Correspondence: Anne Forand, PhD, Centre de Recherche en Myologie, Sorbonne Université, UMRS974, INSERM, Institut de Myologie-Faculté de Médecine de la Pitié Salpêtrière, 105 boulevard de l'Hôpital, 75013 Paris, France.
E-mail: anne.forand@inovarion.com

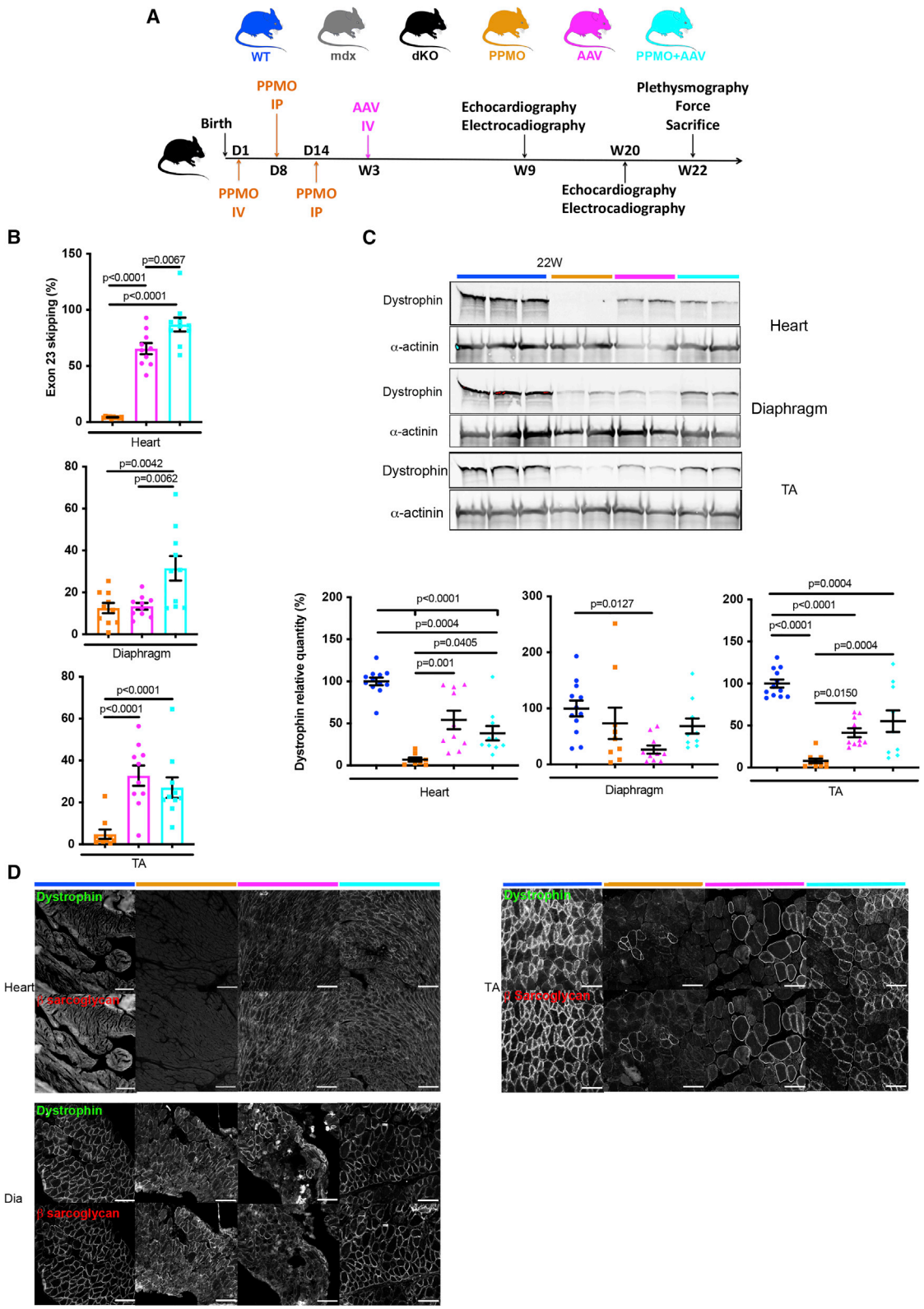

(legend on next page)

therapeutic benefits in skeletal muscles, and they have been reported to have only weak effects on dystrophin restoration in the heart.[16]

Exon skipping can also be mediated by antisense sequences inserted into the small nuclear RNA-U7 and carried by an AAV (adeno-associated virus) vector, AAV-U7. This gene-therapy strategy ensures the continuous production of antisense RNA in dystrophin-deficient murine models[9,17] and in dystrophin-deficient Golden Retriever muscular dystrophy (GRMD) dogs.[18–20] In all dystrophic models, a one-shot treatment with AAV-U7 was sufficient to achieve the restoration of significant levels of dystrophin, associated with an improvement of the muscle force.[9,17,19,20]

Another therapeutic approach for DMD using AAV vectors aims to transfer a shortened cDNA into the cells to mediate the production of a microdystrophin. This strategy has been shown to be effective in a large-animal model of DMD (GRMD) in which intravenous (i.v.) delivery without immunosuppression led to a significant sustained increase in microdystrophin levels in skeletal muscles and improvements in dystrophic symptoms over a period of more than 2 years.[21] Three clinical trials of the AAV-based delivery of microdystrophins (ClinicalTrials.gov: NCT03368742, Solid Biosciences; NCT03375164, Sarepta Therapeutics; and NCT03362502, Pfizer) are currently underway, and the preliminary data suggest that gene therapy is a powerful means of addressing the unmet needs in DMD and the major limitations on the use of this approach. Chief among these limitations is pre-existing anti-capsid immunity, which is an exclusion criterion for AAV gene therapy.[22,23] In other cases in which such immunity develops after treatment, it prevents the readministration of the vector. This is a crucial limitation, as it restricts the sustainability of therapeutic benefit in a context of growth in patients with muscular dystrophy. However, despite the reported efficacy of single injection of AAV-U7 in animal models of DMD,[17,19,20] losses of the viral genome and of therapeutic benefit over time have been observed in treated muscles.[24]

One way of getting around these shortcomings is to combine multiple therapies to maximize efficacy through additive effects of the various approaches. Strategies of this type have proven successful for cultured cells and in clinical practice for other indications.[25,26] A previous study on DMD showed that intramuscular pretreatment with PPMOs targeting dystrophin improved AAV vector maintenance, resulting in 10-fold higher levels of dystrophin protein in the skeletal muscle of mdx mice.[27] Here, we evaluated the benefits of combined treatment over the entire musculature, including vital organs, such as the heart and diaphragm, following the systemic administration of a combination of PPMO and AAV-U7 in dystrophin-utrophin double-knockout mice (dKO), which have a severe dystrophic phenotype. Unlike mdx mice, which have histological signs of muscular dystrophy but few signs of muscle weakness and a relatively normal lifespan, dKO mice develop severe and progressive muscle wasting, leading to heart and diaphragm dysfunction and premature death, mirroring the symptoms of patients with DMD.[28]

The systemic injection of high doses of AAV-U7 (1 + E13 viral genomes) into dKO mice at the age of 3 weeks has been shown to improve survival.[17] For evaluation of the benefits of combination with PPMO pretreatment, a suboptimal dose of AAV-U7 was delivered intravenously. Early exon-skipping treatment, administered at an age when the phenotype is mild or absent, has been shown to prevent DMD progression.[29] We therefore chose to treat mice, at birth, with the dose of PPMO used in a previous study.[30] We also performed three repeated injections of PPMO to prevent a waning of the therapeutic effect during the growth of the animal between birth and the age of 3 weeks. The route of administration seems to be important for targeting specific tissues.[31] We therefore injected PPMO into the animals both intravenously and intraperitoneally (i.p.). Indeed, i.p. injections of PPMO have been shown to induce exon skipping in the diaphragm and skeletal muscles, whereas i.v. injection targets the cardiac and skeletal muscles.[32–34] Taking all of these previous findings into account, we designed this study to determine whether combined treatments have therapeutic potential (Figure 1A). Our findings highlight the major benefits of this combined treatment in the striated muscles and for heart and diaphragm structure and function and demonstrate an unprecedented increase in survival, paving the way for the development of this approach for use in DMD treatment.

RESULTS

Combined PPMO + AAV-U7 Treatment Is Highly Effective for Inducing Exon Skipping and Restoring Dystrophin Expression

dKO mice received intravenous injections of PPMO during the neonatal period and AAV-U7 at the age of 3 weeks. They were compared with dKO mice receiving only one of these treatments (Figure 1A). The efficacy of PPMO + AAV-U7 treatment was first evaluated by quantifying exon skipping. PPMO + AAV-U7-treated mice had higher rates of exon skipping in the heart and diaphragm than mice receiving single treatments, from the age of 22 weeks onward (Figure 1B), and no skipping was observed in untreated wild-type (WT) mice (not shown). These higher rates of exon skipping were correlated with the restoration of dystrophin production in the heart of PPMO + AAV-U7- and AAV-U7-treated mice and in the diaphragm of PPMO + AAV-U7- and PPMO-treated mice (Figure 1C).

Figure 1. Combined PPMO + AAV-U7 Treatment Induces Efficient Exon Skipping and Dystrophin Protein Restoration in the Heart and Diaphragm

(A) Schematic diagram of the treatments administered to the dKO mice: PPMO, AAV-U7, and PPMO + AAV-U7. IV, intravenous; IP, intraperitoneal; D, day; W, week. (B) Quantification of exon 23 skipping in heart, diaphragm, and tibialis anterior (TA) from 22-week-old dKO mice treated with AAV-U7 or with PPMO + AAV-U7. Each dot represents one mouse. The data shown are means ± SEM for 10 mice per group. The significance of differences was determined by one-way ANOVA. (C) Representative immunoblots showing dystrophin levels in the heart, diaphragm, and TA from 22-week-old treated and wild-type (WT) mice; α-actinin is shown as a loading control. The results shown are mean ± SEM for 10 mice per group. The significance of differences was determined by one-way ANOVA. (D) Micrographs showing dystrophin and β-sarcoglycan labeling in the heart, diaphragm (Dia), and TA of 22-week-old WT and treated dKO mice. Scale bars, 100 μm.

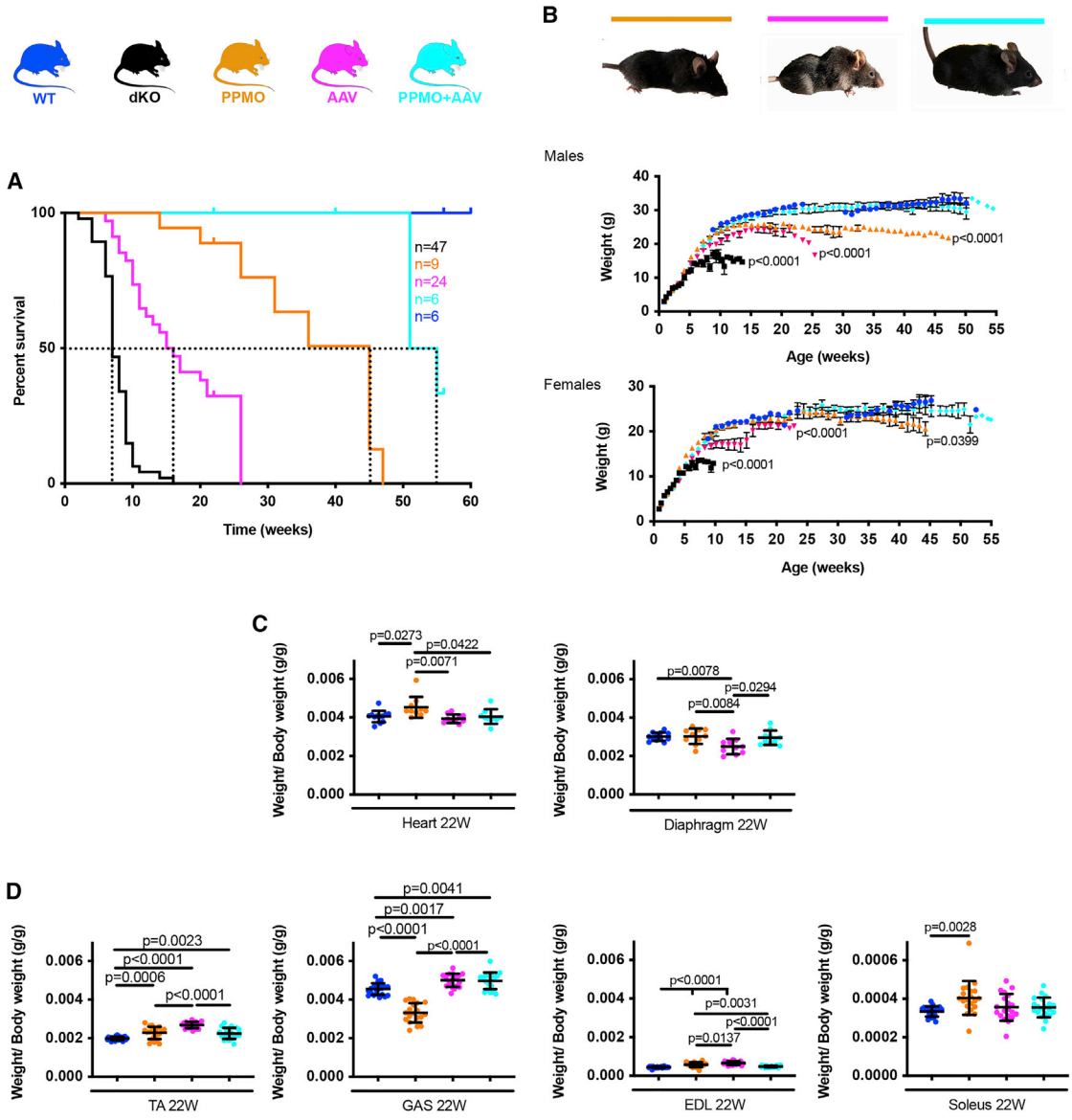

Figure 2. The Combined Approach Extends Survival in dKO Mice

(A) Survival for untreated and treated dKO mice. The survival curves are significantly different, $p < 0.0001$, Mantel-Cox log-rank test. (B) Gross morphology of 22-week-old dKO mice treated with PPMO, AAV-U7, or PPMO + AAV-U7. Comparison of body weight between mice from the different groups during the course of the disease. The data shown are as means ± SEM (n = 10 per group), and significance was determined by one-way ANOVA. Significant differences relative to the WT are indicated. (C and D) Ratios of heart or diaphragm (C) or skeletal (D) muscle weight to body weight for 22-week-old WT and treated dKO mice. The data shown are mean ± SEM for 10 mice per group. Significance was determined by one-way ANOVA.

In skeletal muscles, levels of exon skipping and dystrophin production were similar for PPMO + AAV-U7- and AAV-U7-treated mice but higher in these mice than in PPMO-treated mice (Figures 1B and 1C and S1A and S1B). Furthermore, for all treatments, the restoration of dystrophin expression and its correct localization resulted in a stabilization of the glycoprotein complex at the plasma membrane, as shown by coimmunostaining dystrophin and β-sarcoglycan (Figure 1D).

Combined Treatment Significantly Extends Survival in dKO Mice

Untreated dKO mice died prematurely (median survival of 7 weeks), whereas lifespan was prolonged in all treated mice. The combined treatment resulted in significantly longer survival than either PPMO or AAV-U7 treatment alone (median survival rates of 53, 45, and 15.5 weeks, respectively; Figure 2A). Furthermore, the mice treated with both PPMO and AAV-U7 had a healthier appearance than those treated with either PPMO or AAV alone (Figure 2B).

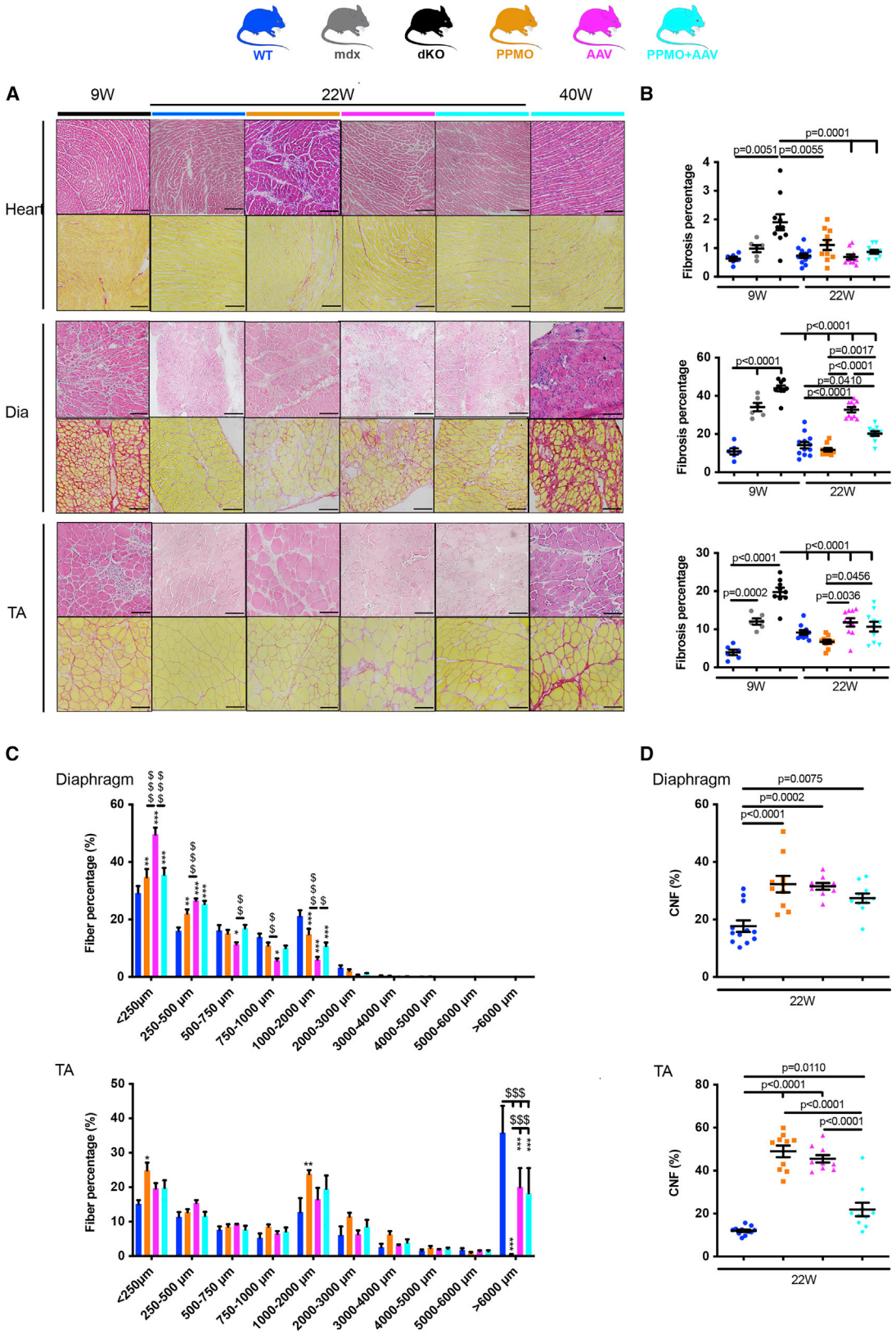

(legend on next page)

The combined treatment restored weight gain to normal levels in both males and females (Figure 2B). It also normalized the ratios of diaphragm and heart weights to body weight (Figure 2C). However, the diaphragm-to-body weight ratio was lower in AAV-U7-treated mice, and the heart-to-body weight ratio was higher in PPMO-treated dKO mice (Figure 2C), suggesting that these treatments had different tissue-specific effects. The ratio of skeletal muscle weight to body weight was heterogeneous in the treated mice (Figure 2D), consistent with the observed dystrophin expression (Figures 1C and S1B).

Combined Treatment Protects dKO Muscles against Fibrosis and Inflammation

Fibrosis is a hallmark of DMD.[3] We therefore analyzed collagen levels by staining muscle cross-sections with sirius red (Figure 3A) and assessing collagen 1 (*Col1a2*) gene expression (Figure S2). Fibrosis levels were lower in all striated muscles from 22-week-old mice treated with PPMO + AAV-U7 than in dKO controls (Figures 3A and S2). We then evaluated inflammation, a secondary consequence of damage to muscle fibers,[35] by analyzing hematoxylin and eosin-stained cross-sections (Figure 3A) and quantifying macrophage-specific (F4/80) and B lymphocyte-specific (cluster of differentiation [CD] 45) transcripts (Figure S2). Lower levels of infiltration (Figure 3A) and slightly lower levels of F4/80 and CD45 expression were observed in the diaphragm and tibialis anterior (TA) of dystrophic mice treated with PPMO + AAV-U7 than in those of dKO controls (Figure S2). Another secondary pathological process superimposed on the chronic proinflammatory state is the segmental degeneration and regeneration of myofibers, leading to an increase in the proportion of small fibers and a higher percentage of centrally located nuclei.[36] An analysis of the distribution of fiber size revealed a partial restoration of muscle fiber size (Figure 3C) associated with a decrease in the percentage of centrally nucleated fibers (Figure 3D) in the diaphragm and TA of mice treated with PPMO + AAV-U7.

Combined Treatment Protects Both Cardiac and Respiratory Functions

The left-ventricular end-diastolic diameter was smaller, and fractional shortening was greater in AAV-U7- and PPMO + AAV-U7-treated mice than in untreated dKO mice, reaching values similar to those in WT mice (Table 1). PPMO treatment alone did not improve cardiac dilation and contractile function. The levels of expression of the *Myh7* and *Nppa* genes, encoding the myosin heavy chain and atrial natriuretic precursor, respectively, were low in the hearts of AAV-U7- and PPMO + AAV-U7-treated mice (Figure 4A). These genes have been shown to be upregulated in cardiomyopathy.[37–39] Duchenne patients develop cardiac conduction defects (e.g., prolonged QRS interval), indicative of a risk of atrio-ventricular block.[40] We therefore monitored cardiac electrical activity in the mice by electrocardiography (ECG). None of the 9-week-old dKO mice subjected to the various treatments had a prolonged QRS interval (Table 1). QRS duration increased over time in PPMO-treated mice (Table S1). Prolonged QRS intervals have been correlated with connexin 43 (Cx43) remodeling in the heart of mdx and dKO mice, and in the hearts of DMD patients.[41] We hypothesized that restoring Cx43 levels at cell-to-cell junctions ensured correct cardiac conduction in dKO mice treated with AAV-U7 alone or with PPMO + AAV-U7. Fluorescence microscopy analysis revealed the restoration of Cx43 localization at intercalated discs in the hearts of dKO mice treated with PPMO + AAV-U7, resulting in a distribution similar to that in WT animals (Figure 4B).

The 9-week-old untreated dKO mice had minute ventilation (V_E) values similar to those of mdx and WT animals (Figure 4C). However, respiratory frequency (*f*R) was higher and was, at this stage, compensated by a low tidal volume (V_T) (Figure 4C), confirming previous reports.[42] At 22 weeks, the V_E of dKO mice treated with PPMO or PPMO + AAV-U7 was similar to that in WT mice. The AAV-U7-treated mice had a higher V_E due to their higher *f*R, which was not compensated by V_T modulation at this time point. The beneficial effect of PPMO + AAV-U7 persisted for at least 40 weeks (Figure 4C). These effects were correlated with higher levels of dystrophin and a reversal of fibrosis, together with a decrease in the expression of inflammatory markers in the diaphragm, as observed for the PPMO and PPMO + AAV-U7 treatments relative to AAV-U7 treatment at 22 weeks.

We then investigated the benefits of the various treatments for skeletal muscle function. Specific maximal force and force drop were evaluated by measuring TA muscle contraction *in situ* in response to nerve stimulation (Figure 4D). Specific maximal force in the TA was greater in mice treated with PPMO + AAV-U7 than in those receiving single treatments (Figure 4D). Force drop, corresponding to susceptibility to contraction-induced injury, was smaller for all treated dKO mice than for mdx mice but remained significantly greater than that in wild-type mice (Figure 4D).

Long-Term Effects of the Combined PPMO + AAV-U7 Treatment

All of the treated dKO died during the study (Figure 2A). We therefore assessed the long-term maintenance of the therapeutic effect. Between 22 and 40 weeks, a loss of the AAV genome was observed in all striated muscles, although levels remained higher in the hearts of PPMO + AAV-U7-treated dKO mice (Figures 5A and S3A). No

Figure 3. The Combined Approach Protects dKO Muscles from Fibrosis and Inflammation

(A) Representative micrographs of hematoxylin-eosin- and sirius red-stained sections of heart, diaphragm, and TA from the indicated groups of mice. Scale bars, 100 μm. (B) Fibrosis calculated as a percentage of the total area with ImageJ software, from sirius red-stained sections from 22-week-old mice. The data shown are means ± SEM of at least six mice per group, and significance was determined by one-way ANOVA. (C and D) Fiber size distribution (C) and percentage of centrally nucleated fibers (D) calculated with MuscleJ software after laminin fluorescence staining for the diaphragm (top panel) and TA (bottom panel). The data shown are mean ± SEM for at least 10 mice per group, and significance was determined by one-way ANOVA (*$p < 0.05$, **$p < 0.01$, ***$p < 0.001$ relative to WT mice; \$$p < 0.05$, \$\$$p < 0.01$, \$\$\$$p < 0.001$ relative to other treated mice).

Table 1. Cardiac Function Parameters

	WT 9W		mdx 9W		dKO 9W		PPMO 9W		AAV-U7 9W		PPMO + AAV-U7 9W	
Time (ms)	97	±0.4	114.4	±4.9	136.2	±7.4***	109.2	±1.8$^{\$\$\$}$	108	±1.5$^{\$\$\$}$	100.4	±1.4$^{\$\$\$}$
Heart rate (bpm)	618.5	±2.9	529.1	±21.3**	468.1	±14.1***	553.2	±8.4$^{***,\$\$\$}$	558	±7.9$^{**,\$\$\$}$	599.8	±8.0$^{\$\$\$,\#\#}$
FS (%)	46	±0.4	44.2	±0.4	39.8	±1.7*	38.7	±1.2**	45.1	±0.5$^{\$,\#\#\#}$	43.6	±0.8$^{\#}$
LVDd/body weight (cm/g)	0.017	±0.0004	0.013	±0.0005$^{\#}$	0.021	±0.0002***	0.016	±0.0003$^{\$\$\$}$	0.017	±0.0005$^{\$\$\$}$	0.016	±0.0004$^{\$\$\$}$
HR (bpm)	748.7	±5.5	576.4	±34.5***	536.7	±24.3***	667.8	±12.0$^{**,\$\$\$}$	627.1	±12.4$^{***,\$\$}$	698.9	±9.9$^{\$\$\$}$
RR (ms)	80.2	±0.6	106.7	±7.0**	119.4	±7.3***	90.9	±1.8$^{*,\$\$\$}$	97.5	±2.1$^{\$\$\$}$	86.3	±1.3$^{\$\$\$}$
PR (ms)	34.3	±0.5	35.9	±1.8	32.4	±1.8	33.7	±0.6	33.5	±0.5	33.0	±0.7
QRS (ms)	10.3	±0.1	12.6	±1.8	18.1	±1.1***	12.0	±0.2$^{\$\$\$}$	11.7	±0.3$^{\$\$\$}$	11.5	±0.2$^{\$\$\$}$

Parameters measured by echocardiography and on electrocardiograms in 9-week-old mice. The data shown are mean ± SEM for at least 10 mice (except for mdx mice; n = 5 for echocardiography and n = 4 for ECG). Significance was determined by one-way ANOVA with correction for multiple testing. bpm, beats per minute; HR, heart rate.
*p < 0.05, **p < 0.01, ***p < 0.001 versus WT mice.
$^{\$}$p < 0.05, $$p < 0.01, $$$p < 0.001 versus untreated dKO mice.
$^{\#}$p < 0.05, ##p < 0.01, ###p < 0.001 versus PPMO-treated dKO mice.

exon skipping was observed in untreated WT mice (not shown). These findings are consistent with the levels of dystrophin protein measured, which remained stable until 52 weeks in the hearts of dKO mice receiving the combined treatment (Figures 5B–5D), ensuring an absence of cardiac manifestations of the disease (Table S1). Despite the very low AAV genome content (Figure 5A) and very low levels of dystrophin protein (Figure 5B) in the diaphragm, respiratory function remained normal 40 weeks after PPMO + AAV-U7 treatment (Figure 4C). From 45 weeks onward, dystrophin levels decreased significantly (Figures 5D and S3B) and changes in the histological features (Figure 5E) of the diaphragm and skeletal muscle were observed in dKO mice treated with PPMO alone. Finally, 52 weeks post-treatment, only dKO mice that had received the PPMO + AAV-U7 combination remained alive, with dystrophin protein levels in the heart of about 20% of those in WT mice with normal cardiac histology findings (Figures 5D and 5E). Nevertheless, a very weak dystrophin signal was detected in the diaphragm of treated mice (Figure 5D). Accordingly, histological analyses of the diaphragm revealed major inflammation and fibrosis in PPMO + AAV-U7-treated mice (Figure 5E), suggesting that these mice would probably have died from respiratory failure at about 52 weeks post-treatment.

DISCUSSION

We found that the combined PPMO + AAV-U7 treatment was more effective at improving health and extending the lifespan of dKO mice than single treatments. These observed benefits can be explained by considering the results obtained with single PPMO or AAV-U7 treatments.

PPMO was first administered to newborns by i.v. injection (Figure 1A) and would certainly have been diluted during tissue growth, as demonstrated by the low rates of dystrophin rescue observed in the hearts of 3-week-old-treated mice (data not shown). However, PPMO was then readministered by the i.p. route, explaining the strong restoration of dystrophin levels in the diaphragm (data not shown). In the single AAV-U7 approach, dystrophin levels were effectively restored in the heart but not in the diaphragm; the lifespan of these mice was extended by more than 25 weeks, whereas survival for more than 45 weeks was reported for AAV-U7-treated dKO mice in a previous study.[30] This difference may be accounted for by the differences in AAV dose used. We deliberately used a dose of AAV known to be suboptimal to create the best possible experimental conditions for evaluating the benefits of the combined approach.

An analysis of the benefits of treatment in 22-week-old mice showed that AAV-U7 alone was the least effective treatment over time. Indeed, survival was 89% for mice treated with PPMO alone, but only 32% for mice treated with AAV alone (Figure 1B). Nevertheless, the surviving mice had similar rates of exon skipping in the diaphragm, regardless of the type of single treatment they had received (Figure 1B). Dystrophin protein levels were also similar for the two single treatments (Figure 3C). However, histological sections revealed significantly lower levels of fibrosis in the diaphragm in mice treated with PPMO alone than in those treated with AAV alone (Figure 3B). Moreover, diaphragm function was impaired in the AAV group, whereas it was similar to that in the WT in the PPMO group. Thus, despite similar rates of exon skipping and protein levels in the diaphragm in the mice of the AAV and PPMO groups, histological and functional results were better for the PPMO group than for the AAV group. These differences may reflect differences in the time course of treatment. Indeed, dystrophin expression was restored earlier in the PPMO group (injections on day [D] 1 , D8, and D14) than in the AAV group, in which the treatment was administered at 3 weeks of age (Figure 1A). The timing of dystrophin protein restoration is crucial for the prevention of disease progression. These findings confirm a previous report of the prevention of DMD progression by an early exon-skipping therapy, administered at an age at which the phenotype was absent or mild.[29]

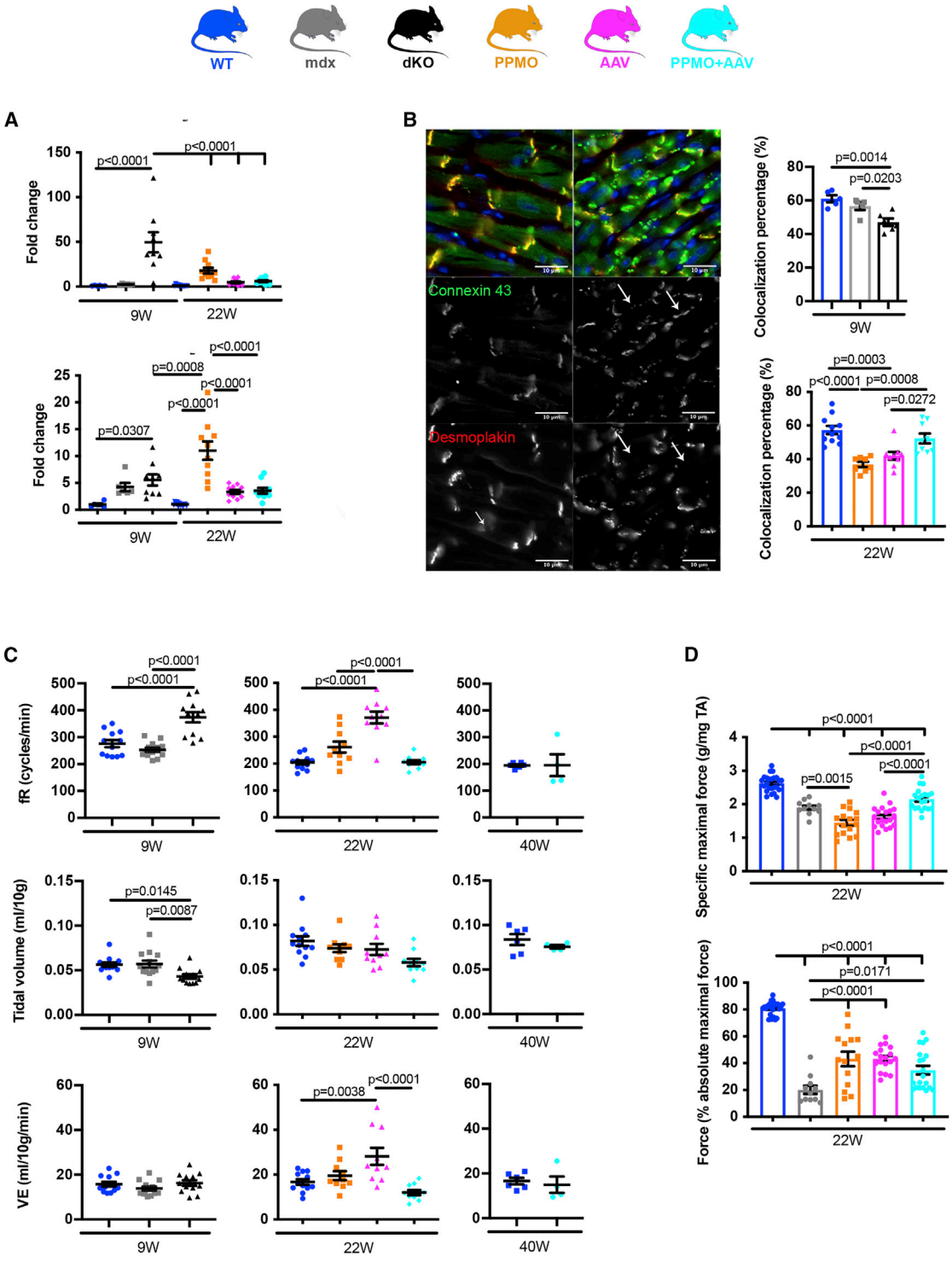

Figure 4. The Combined Approach Restores Normal Cardiac and Respiratory Functions and Improves Skeletal Muscle Function

(A) RT-quantitative real-time PCR analysis of *Myh7* and *Nppa* expression in the hearts of 9-week-old WT, mdx, and untreated dKO mice and 22-week-old WT mice and dKO mice treated with PPMO, AAV-U7, or PPMO + AAV-U7. The data shown are mean ± SEM for at least 10 mice per group, and significance was determined by one-way ANOVA. (B) Micrographs showing connexin 43 and desmoplakin labeling in the heart for 9-week-old WT and dKO mice. 4′,6-Diamidino-2-phenylindole (DAPI) counter-staining (blue) of the nuclei. Arrows indicate the lateralization of connexin 43. Scale bars, 10 μm. The colocalization of connexin 43 and desmoplakin was quantified for the

(legend continued on next page)

An evaluation of cardiac function revealed a smaller left-ventricular end-diastolic diameter and greater fractional shortening in AAV-U7-treated mice than in untreated dKO mice. The values obtained were similar to those for WT mice (Table 1). By contrast, PPMO treatment alone had no beneficial effect on cardiac dilation and contractile function. Overall, these data show that at 22 weeks of age, mice treated with AAV-U7 alone have poor respiratory function and normal cardiac function, whereas mice treated with PPMO alone have normal diaphragm function and abnormal cardiac parameters.

The benefits of the PPMO pretreatment can also be evaluated by comparing the AAV-U7 and PPMO + AAV-7 groups. These two groups had similar viral genome levels at 22 weeks post-treatment (Figure S3) but significantly different phenotypes (Figure 3A). We suggest that this difference may be the result of PPMO pretreatment in the PPMO + AAV-U7 group, resulting in early dystrophin production, decreasing inflammation in the target tissues, as previously described.[43] This would result in more appropriate conditions for vector trafficking or vector genome (vg) processing, as reported in the liver.[44]

Only mice treated with PPMO alone or with the PPMO + AAV-U7 combination were still alive at 40 weeks, again suggesting that the preservation of diaphragm function is important for the survival of the treated mice. Nevertheless, histological analyses at this time point revealed dystrophic features of the diaphragm in the PPMO group, probably due to PPMO clearance of a loss of dystrophin protein production. Nevertheless, the cause of death in these mice was cardiac dysfunction, as revealed by echocardiography and ECG parameters (Table S1).

The combination of PPMO and AAV-U7 treatments therefore seems to combine the benefits of these two individual approaches in a complementary manner, resulting in the rescue of respiratory function by PPMO and of cardiac function by AAV-U7 (Figure 6). However, even though the combined treatment significantly decreased both the cardiac and respiratory dysfunctions that prove fatal in DMD patients, our data strongly suggested that the PPMO + AAV-U7-treated dKO mice would be likely to die after about 1 year from respiratory failure, due to loss of the therapeutic effects of PPMO. Additional preclinical optimizations are therefore required for this therapeutic approach. We propose the upgrading of the treatment protocol for the PPMO + AAV-U7 combination, with the addition of regular readministrations of PPMO, made possible by the lack of immunogenicity of this treatment.

Genomic editing is one of the most promising new strategies developed to date for DMD.[7,8,45] However, CRISPR, even with optimized guide RNAs or nucleases, can nevertheless modify the genome in unintended ways. Technical advances in genome editing will therefore be required before this approach can be developed for clinical use. For this reason and given the urgent need for more effective therapeutic solutions for Duchenne patients, improvements to existing approaches are required. The most promising approach currently available is microdystrophin gene therapy, which can be used in all DMD patients, regardless of genotype, whereas exon-skipping strategies are more personalized, depending on the exons to be skipped, but can restore the production of almost full-length dystrophin molecules, conferring superior functional benefits. We have already shown that PPMO pretreatment increases the benefits of AAV-mediated microdystrophin cDNA transfer into mdx muscles.[27] Based on the results presented here, we can propose a protocol based on the use of a combination of PPMO and AAV-microdystrophin, with the regular readministration of PPMO to ensure long-lasting benefits of gene therapy. This combined strategy therefore constitutes a therapeutic breakthrough, providing unprecedented benefits for the long-term treatment of DMD.

METHODS

Vector Production

A three-plasmid (pscAAV-U7Ex23, pXX6, and pAAV9pITRCO2) transfection protocol was used with. Vector particles were purified from lysates obtained 48 h after transfection on iodixanol gradients, and titers were determined by real-time PCR and expressed as vg per milliliter.

Animal Care

Animals were housed at the Myology Research Center (Paris, France) under 12 h/12 h light/dark conditions, with *ad libitum* access to food and water. The experiments performed were authorized and approved by the local institutional review board (2016071210565236).

WT mice were obtained from Janvier Laboratories. We generated dKO and mdx mice by crossing ($Utr^{+/-}$; $Dys^{-/-}$) mice (JB10ScSn.Cg-Utrntm1KedDmdmdx/J; Jackson Laboratory, Bar Harbor, ME, USA). We injected 25 mg/kg PPMO (Pip9b2-PMO conjugate[46]) i.v. into the temporal vein on day 1 and i.p. on day 8. The dKO mice then received retro-orbital injections (i.v.) of 1E+12 vg of self complementary scAAV9-U7Ex23 under general anesthesia, at the age of 3 weeks. We selected a minimum of 20 mice (male/female ratio: 50/50) at random for each treatment group. Ten were killed at 22 weeks (male/female ratio: 50/50) of age for molecular analysis, and the other 10 were retained for survival analysis. Four of the mice kept for survival (2 males and 2 females) in the PPMO + AAV group were

various groups of mice at the age indicated. Significance was determined by one-way ANOVA. (C) Respiratory parameters for 9-week-old WT (n = 12), mdx (n = 13), and dKO (n = 13) mice; 22-week-old WT (n = 12), PPMO-treated (n = 10), AAV9-U7-treated (n = 10), and PPMO + AAV9-U7-treated (n = 10) dKO mice; and 40-week-old WT (n = 6) and PPMO + AAV9-U7-treated (n = 4) dKO mice *f*R, respiratory frequency; V_T, tidal volume; V_E, minute ventilation. The data shown are means ± SEM. Significance was determined by one-way ANOVA for 22-week-old mice and with unpaired t tests for 40-week-old mice. (D) Specific maximal force and force drop resulting from the injury induced by 10 lengthening contractions of the TA for 22-week-old WT, mdx, and treated dKO mice. The data shown are mean ± SEM for at least 10 mice per group, and significance was determined by one-way ANOVA.

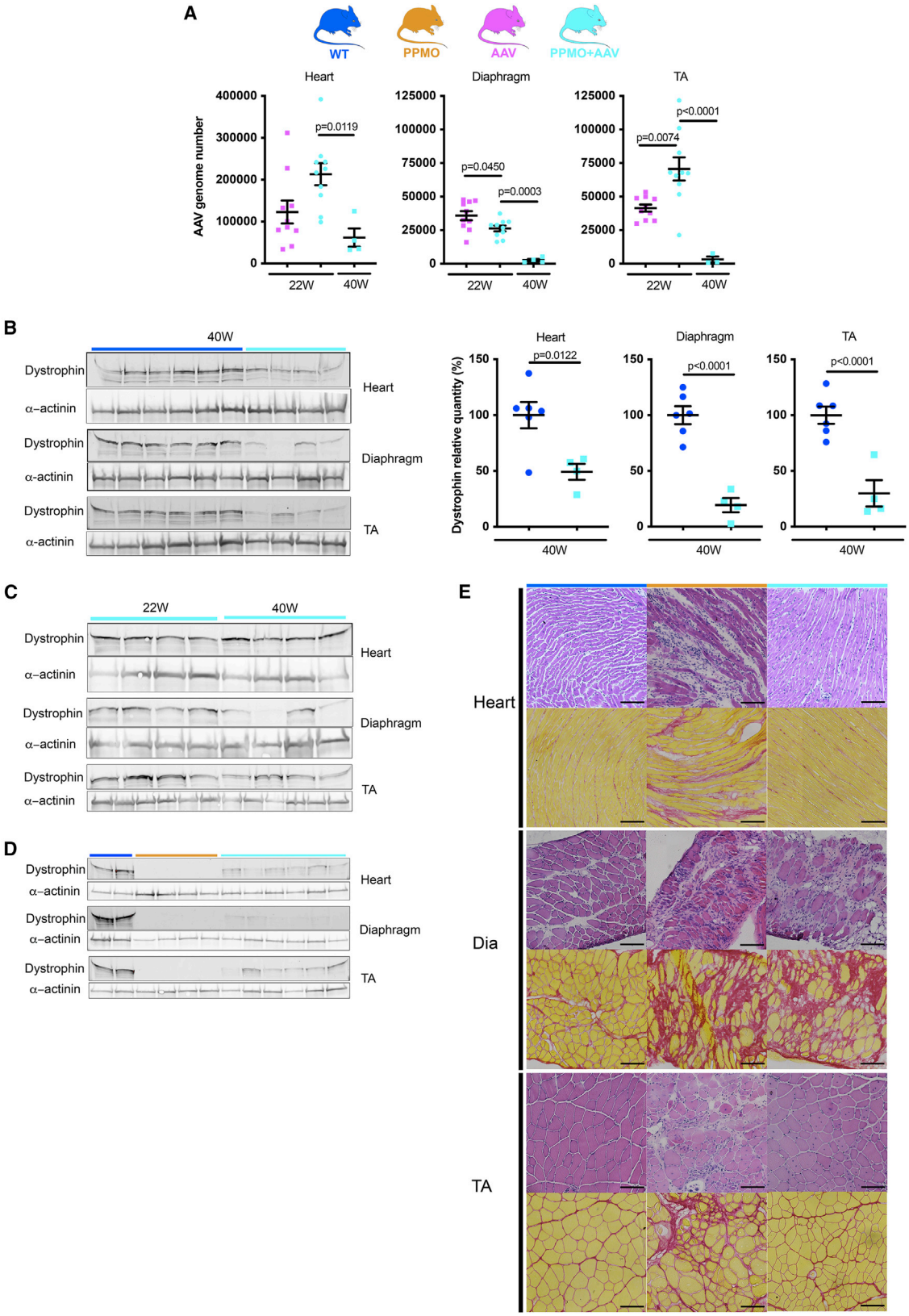

(legend on next page)

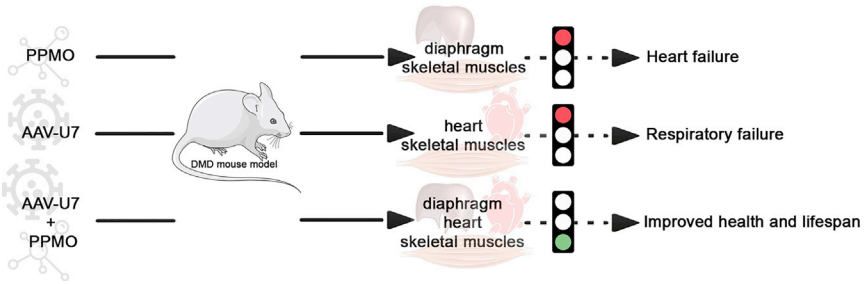

Figure 6. Schematic Diagram of the Benefits of the Different Treatments in Striated Muscles

killed at the age of 40 weeks for molecular analysis. The mice used for the survival analysis were killed at a humane end point at which their weight had decreased by more than 10% or as required by ethical rules. Their muscles were collected, snap frozen in liquid nitrogen-cooled isopentane, and stored at −80°C.

Quantification of AAV Genome Content

Genomic DNA was extracted from mouse muscles with the Puregene Blood kit (QIAGEN, Hilden, Germany). AAV genome copy number and genomic DNA were determined on 100 ng of genomic DNA by absolute quantitative real-time PCR on a StepOnePlus system (Applied Biosystems, Foster City, CA, USA) with TaqMan Universal Master Mix (Applied Biosystems, Foster City, CA, USA). The primers (forward: 5′-CTCCATCACTAGGGGTTCCTTG-3′ and reverse: 5′-GTAGATAAGTAGCATGGC-3′) and probe (5′-TAGTTAATGA TTAACCC-3′) were selected for specific amplification of the vector genome sequence. As a reference sample, we generated 10-fold serial dilutions (from 10^7 to 10^1 copies) of a preparation of the pAAV plasmid. All genomic DNA samples were analyzed in duplicate.

Exon-Skipping Analysis

Total RNA was isolated from mouse muscles with NucleoSpin RNA II (Macherey-Nagel, Hoerdt, France) and reverse transcription (RT) performed on 20 ng of RNA with Superscript II and random primers (Life Technologies, Carlsbad, CA, USA). Nonskipped and skipped dystrophin transcripts were detected by quantitative PCR, as previously described.[17]

Western Blot Analysis

Protein extracts were obtained from pooled muscle sections treated with 125 mM sucrose, 5 mM Tris-HCl, pH 6.4, 6% XT Tricine Running Buffer (Bio-Rad, Hercules, CA, USA), 10% SDS, 10% glycerol, and 5% β-mercaptoethanol. The samples were purified with the Pierce Compat-Able Protein Assay Preparation Reagent Set (Thermo Scientific, Waltham, MA, USA), and total protein concentration was determined with the Pierce BCA Protein Assay Kit (Thermo Fisher Scientific, Waltham, MA, USA). The samples were denatured by heating at 95°C for 5 min, and 100 μg of protein was subjected to electrophoresis in a Criterion XT Tris-acetate precast 3%–8% polyacrylamide gel (Bio-Rad, Hercules, CA, USA). The membrane was probed with monoclonal primary antibodies directed against dystrophin (NCL-DYS1, 1:50; Leica Biosystems, Nanterre, France) and α-actinin (1:1,000; Sigma-Aldrich) and was then incubated with a goat anti-mouse secondary antibody (StarBright Blue 700 conjugated; 1:5,000) for imaging with the Chem-iDocMP Imaging System (Bio-Rad, Hercules, CA, USA). Band intensity was quantified with Image Lab software, with the mean intensity obtained for the WT taken as 100%.

Immunohistochemistry and Histology

Tissue sections (10 μm thick) were cut and stained with hematoxylin and eosin for the assessment of overall muscle morphology. Collagen fibers were detected by sirius red staining. Sections were fixed by incubation for 10 min with 4% formaldehyde and dried. They were then incubated with a 0.3% solution of sirius red in aqueous saturated picric acid for 1 h, washed in acidified water (0.5% acetic acid), dehydrated, and mounted in VectaMount (Vector Laboratories, Peterborough, UK). Fibrosis was then quantified in a nonblind manner by determining the proportion of the total cross-sectional area stained red with ImageJ software.

We then assessed dystrophin levels on cryosections by incubation with the Lab Vision Dystrophin (1:500; Thermo Scientific, Waltham, MA, USA) rabbit polyclonal antibody and β-sarcoglycan expression by incubation with a monoclonal antibody against this protein (1:50; Novocastra, Newcastle, UK). The binding of primary antibodies was detected by incubation with an Alexa 488-conjugated donkey anti-rabbit secondary antibody (1:1,000; Life Technologies, Carlsbad, CA, USA) and an Alexa 594-conjugated goat anti-mouse

Figure 5. Long-Term Combined PPMO + AAV-U7 Treatment

(A) Quantification of the number of vector genomes in the heart, diaphragm, and tibialis anterior (TA) of AAV-U7- and PPMO + AAV-U7-treated mice. The data shown are mean ± SEM for 10 mice per group at 22 weeks of age and four mice at 40 weeks of age. Significance was determined by one-way ANOVA. (B) Representative immunoblots and quantification of dystrophin and α-actinin in striated muscles from WT (dark blue) and PPMO + AAV-U7-treated dKO mice (light blue) at 40 weeks of age. The data shown are means ± SEM for 6 WT and 4 PPMO + AAV-treated dKO mice. Significance was determined in unpaired t tests. (C) Representative cropped immunoblots of dystrophin and α-actinin for the heart, diaphragm, and TA of PPMO + AAV-U7-treated dKO mice at 22 and 40 weeks of age. (D) Representative immunoblots of dystrophin and α-actinin for the heart, diaphragm, and TA of WT (50 weeks old) mice and dKO mice treated with PPMO (about 45 weeks old) or PPMO + AAV-U7 (about 52 weeks old) at the humane endpoint. (E) Staining with hematoxylin and eosin and sirius red of heart, diaphragm (Dia), and TA sections from WT mice and from PPMO- and PPMO + AAV-U7-treated dKO mice at about 50, 45, and 52 weeks of age, respectively.

secondary antibody (1:1,000; Life Technologies, Carlsbad, CA, USA). The monoclonal antibody was used with the M.O.M. kit (Vector Laboratories, Peterborough, UK).

Muscle-Function Assessments

Specific force and force drop (a measure of susceptibility to contraction-induced injury) were evaluated by measuring the contraction of the TA muscle in response to nerve stimulation *in situ*, as previously described.[47] The investigators were blind to treatment allocation and outcome assessment. Mice were anesthetized with 100 μL/20 g body weight of a mixture of ketamine (100 mg/mL) and xylazine (20 mg/mL). Body temperature was maintained at 37°C with radiant heat. The knee and foot were fixed with pins and clamps, and the distal tendon of the muscle was attached to a lever arm in a servomotor system (305B, Dual-Mode Lever; Aurora Scientific, Aurora, Canada) with a silk ligature. The sciatic nerve was proximally crushed and distally stimulated by a bipolar silver electrode with supramaximal square wave pulses of 0.1 ms duration (10 V). We measured the absolute maximal force generated during isometric tetanic contractions in response to electrical stimulation (150 Hz, 500 ms). Absolute maximal force was determined at L0 (the length at which maximal tension was obtained during the tetanus). Absolute maximal force was normalized against muscle weight as an estimate of specific maximal force (absolute maximal force/muscle weight).

Susceptibility to contraction-induced injury was estimated by determining the force drop resulting from lengthening contraction-induced injury. The sciatic nerve was stimulated for 700 ms (frequency of 125 Hz). A maximal isometric contraction of the TA muscle was initiated during the first 500 ms. Muscle lengthening (10% L0), at a velocity of 5.5 mm/s (0.85 fiber lengths/s), was then imposed during the last 200 ms. Nine lengthening contractions of the muscle were performed, each separated by a 45-s rest period. All contractions were performed at an initial length L0. The data were recorded with the Powerlab 8/36 data acquisition system (AD Instruments, Sydney, Australia). Maximal force was measured for each contraction and expressed as a percentage of the initial maximal force.

Echocardiography

Mice were lightly anesthetized with 0.2%–0.5% isoflurane in O_2 and placed on a heating pad (37°C). Echocardiography was performed with a probe emitting ultrasound at a frequency of 9 to 14 MHz (Vivid7 PRO apparatus; GE Medical System, Buc, France) applied to the chest wall. Cardiac ventricular dimensions and fractional shortening were measured in two-dimensional (2D) mode and M-mode. The examinations were performed by an echocardiographer blind to genotype and treatment.

Electrocardiography

Electrocardiograms were recorded for the mice with the noninvasive ecgTUNNEL (Emka Technologies, Paris, France), with minimal filtering. Waveforms were recorded with Iox software, and intervals were measured manually with ECG Auto. The investigators were blind to treatment allocation and outcome assessment.

Measurement of Ventilation

Ventilation was measured in a blind manner, by whole-body flow-through plethysmography. The measurement and reference chambers were connected to a pneumotachograph (Fleisch 0000) connected to a volume transducer (Gould Z46170). Respiratory signals were relayed to a 1401 interface (1401 Plus; Cambridge Electronic Design [CED], UK) and processed with Spike 2 software (6.14; CED, UK). Both fR and V_T were derived from the ventilatory flow signal. Minute ventilation was calculated as follows: $V_E = V_T \times f$R.

Statistical Analysis

All results are expressed as mean values ± SEM. Differences between groups were assessed by one-way ANOVA with multiple comparisons. For two-by-two comparisons, the significance of differences was assessed in unpaired Student's t tests. Welch correction was applied in situations in which the assumption of homogeneous variances was not confirmed.

SUPPLEMENTAL INFORMATION

Supplemental Information can be found online at https://doi.org/10.1016/j.omtm.2020.03.011.

AUTHOR CONTRIBUTIONS

S.L. and F.P.-R. conceived the project, raised funds, and supervised the study. A.F. designed all of the experiments, analyzed the data, and prepared the figures. A.F., A.M., N.M., C.S.-C., and M.L. performed and/or analyzed *in vivo* experiments. A.F., C.P., and C.I. performed molecular experiments. M.W. provided reagents. A.F., A.M., and F.P.-R. wrote the manuscript. A.F., A.M., C.S.-C., N.M., M.L., M.W., F.P.-R., and S.L. revised the manuscript.

CONFLICTS OF INTEREST

The authors declare no competing interests.

ACKNOWLEDGMENTS

The majority of the results of this study were carried out, thanks to a service provision by the company Inovarion. We thank Laura Julien and Sofia Benkhelifa-Ziyyat of the MYOVECTO platform of the Myology Research Center for producing AAV-U7 and Bruno Cadot for his help with image analysis. We thank Kim Nguyen and Olivier Brégerie for animal care. The project and A.F. were funded by Association Française contre les Myopathies AFM-Téléthon and by the Institute of Myology.

REFERENCES

1. Mendell, J.R., Shilling, C., Leslie, N.D., Flanigan, K.M., al-Dahhak, R., Gastier-Foster, J., Kneile, K., Dunn, D.M., Duval, B., Aoyagi, A., et al. (2012). Evidence-based path to newborn screening for Duchenne muscular dystrophy. Ann. Neurol. *71*, 304–313.

2. Campbell, K.P., and Kahl, S.D. (1989). Association of dystrophin and an integral membrane glycoprotein. Nature *338*, 259–262.

3. Morales, J.A., and Mahajan, K. (2018). Dystrophinopathies. StatPearls (StatPearls Publishing), http://www.ncbi.nlm.nih.gov/books/NBK534245/.
4. Gatheridge, M.A., Kwon, J.M., Mendell, J.M., Scheuerbrandt, G., Moat, S.J., Eyskens, F., Rockman-Greenberg, C., Drousiotou, A., and Griggs, R.C. (2016). Identifying Non-Duchenne Muscular Dystrophy-Positive and False Negative Results in Prior Duchenne Muscular Dystrophy Newborn Screening Programs: A Review. JAMA Neurol. *73*, 111–116.
5. Shimizu-Motohashi, Y., Komaki, H., Motohashi, N., Takeda, S., Yokota, T., and Aoki, Y. (2019). Restoring Dystrophin Expression in Duchenne Muscular Dystrophy: Current Status of Therapeutic Approaches. J. Pers. Med. *9*, 1.
6. Nelson, C.E., Wu, Y., Gemberling, M.P., Oliver, M.L., Waller, M.A., Bohning, J.D., Robinson-Hamm, J.N., Bulaklak, K., Castellanos Rivera, R.M., Collier, J.H., et al. (2019). Long-term evaluation of AAV-CRISPR genome editing for Duchenne muscular dystrophy. Nat. Med. *25*, 427–432.
7. Min, Y.-L., Bassel-Duby, R., and Olson, E.N. (2019). CRISPR Correction of Duchenne Muscular Dystrophy. Annu. Rev. Med. *70*, 239–255.
8. Mata López, S., Balog-Alvarez, C., Vitha, S., Bettis, A.K., Canessa, E.H., Kornegay, J.N., and Nghiem, P.P. (2020). Challenges associated with homologous directed repair using CRISPR-Cas9 and TALEN to edit the DMD genetic mutation in canine Duchenne muscular dystrophy. PLoS ONE *15*, e0228072.
9. Goyenvalle, A., Vulin, A., Fougerousse, F., Leturcq, F., Kaplan, J.-C., Garcia, L., and Danos, O. (2004). Rescue of dystrophic muscle through U7 snRNA-mediated exon skipping. Science *306*, 1796–1799.
10. Eder, P.S., DeVine, R.J., Dagle, J.M., and Walder, J.A. (1991). Substrate specificity and kinetics of degradation of antisense oligonucleotides by a 3′ exonuclease in plasma. Antisense Res. Dev. *1*, 141–151.
11. Warfield, K.L., Panchal, R.G., Aman, M.J., and Bavari, S. (2006). Antisense treatments for biothreat agents. Curr. Opin. Mol. Ther. *8*, 93–103.
12. Lu, Q.-L., Yokota, T., Takeda, S., Garcia, L., Muntoni, F., and Partridge, T. (2011). The status of exon skipping as a therapeutic approach to duchenne muscular dystrophy. Mol. Ther. *19*, 9–15.
13. Yokota, T., Lu, Q.-L., Partridge, T., Kobayashi, M., Nakamura, A., Takeda, S., and Hoffman, E. (2009). Efficacy of systemic morpholino exon-skipping in Duchenne dystrophy dogs. Ann. Neurol. *65*, 667–676.
14. Guidotti, G., Brambilla, L., and Rossi, D. (2017). Cell-Penetrating Peptides: From Basic Research to Clinics. Trends Pharmacol. Sci. *38*, 406–424.
15. Tsoumpra, M.K., Fukumoto, S., Matsumoto, T., Takeda, S., Wood, M.J.A., and Aoki, Y. (2019). Peptide-conjugate antisense based splice-correction for Duchenne muscular dystrophy and other neuromuscular diseases. EBioMedicine *45*, 630–645.
16. Verhaart, I.E.C., and Aartsma-Rus, A. (2019). Therapeutic developments for Duchenne muscular dystrophy. Nat. Rev. Neurol. *15*, 373–386.
17. Goyenvalle, A., Babbs, A., Wright, J., Wilkins, V., Powell, D., Garcia, L., and Davies, K.E. (2012). Rescue of severely affected dystrophin/utrophin-deficient mice through scAAV-U7snRNA-mediated exon skipping. Hum. Mol. Genet. *21*, 2559–2571.
18. Bish, L.T., Sleeper, M.M., Forbes, S.C., Wang, B., Reynolds, C., Singletary, G.E., Trafny, D., Morine, K.J., Sanmiguel, J., Cecchini, S., et al. (2012). Long-term restoration of cardiac dystrophin expression in golden retriever muscular dystrophy following rAAV6-mediated exon skipping. Mol. Ther. *20*, 580–589.
19. Vulin, A., Barthélémy, I., Goyenvalle, A., Thibaud, J.-L., Beley, C., Griffith, G., Benchaouir, R., le Hir, M., Unterfinger, Y., Lorain, S., et al. (2012). Muscle function recovery in golden retriever muscular dystrophy after AAV1-U7 exon skipping. Mol. Ther. *20*, 2120–2133.
20. Le Guiner, C., Montus, M., Servais, L., Cherel, Y., Francois, V., Thibaud, J.-L., Wary, C., Matot, B., Larcher, T., Guigand, L., et al. (2014). Forelimb treatment in a large cohort of dystrophic dogs supports delivery of a recombinant AAV for exon skipping in Duchenne patients. Mol. Ther. *22*, 1923–1935.
21. Le Guiner, C., Servais, L., Montus, M., Larcher, T., Fraysse, B., Moullec, S., Allais, M., François, V., Dutilleul, M., Malerba, A., et al. (2017). Long-term microdystrophin gene therapy is effective in a canine model of Duchenne muscular dystrophy. Nat. Commun. *8*, 16105.
22. Aronson, S.J., Veron, P., Collaud, F., Hubert, A., Delahais, V., Honnet, G., de Knegt, R.J., Junge, N., Baumann, U., Di Giorgio, A., et al. (2019). Prevalence and Relevance of Pre-Existing Anti-Adeno-Associated Virus Immunity in the Context of Gene Therapy for Crigler-Najjar Syndrome. Hum. Gene Ther. *30*, 1297–1305.
23. Lorain, S., Gross, D.-A., Goyenvalle, A., Danos, O., Davoust, J., and Garcia, L. (2008). Transient immunomodulation allows repeated injections of AAV1 and correction of muscular dystrophy in multiple muscles. Mol. Ther. *16*, 541–547.
24. Le Hir, M., Goyenvalle, A., Peccate, C., Précigout, G., Davies, K.E., Voit, T., Garcia, L., and Lorain, S. (2013). AAV genome loss from dystrophic mouse muscles during AAV-U7 snRNA-mediated exon-skipping therapy. Mol. Ther. *21*, 1551–1558.
25. Breuel, S., Vorm, M., Bräuer, A.U., Owczarek-Lipska, M., and Neidhardt, J. (2019). Combining Engineered U1 snRNA and Antisense Oligonucleotides to Improve the Treatment of a BBS1 Splice Site Mutation. Mol. Ther. Nucleic Acids *18*, 123–130.
26. Hodgetts, S.I., Yoon, J.H., Fogliani, A., Akinpelu, E.A., Baron-Heeris, D., Houwers, I.G.J., Wheeler, L.P.G., Majda, B.T., Santhakumar, S., Lovett, S.J., et al. (2018). Cortical AAV-CNTF Gene Therapy Combined with Intraspinal Mesenchymal Precursor Cell Transplantation Promotes Functional and Morphological Outcomes after Spinal Cord Injury in Adult Rats. Neural Plast. *2018*, 9828725.
27. Peccate, C., Mollard, A., Le Hir, M., Julien, L., McClorey, G., Jarmin, S., Le Heron, A., Dickson, G., Benkhelifa-Ziyyat, S., Piétri-Rouxel, F., et al. (2016). Antisense pre-treatment increases gene therapy efficacy in dystrophic muscles. Hum. Mol. Genet. *25*, 3555–3563.
28. Deconinck, A.E., Rafael, J.A., Skinner, J.A., Brown, S.C., Potter, A.C., Metzinger, L., Watt, D.J., Dickson, J.G., Tinsley, J.M., and Davies, K.E. (1997). Utrophin-dystrophin-deficient mice as a model for Duchenne muscular dystrophy. Cell *90*, 717–727.
29. Wu, B., Cloer, C., Lu, P., Milazi, S., Shaban, M., Shah, S.N., Marston-Poe, L., Moulton, H.M., and Lu, Q.L. (2014). Exon skipping restores dystrophin expression, but fails to prevent disease progression in later stage dystrophic dko mice. Gene Ther. *21*, 785–793.
30. Goyenvalle, A., Babbs, A., Powell, D., Kole, R., Fletcher, S., Wilton, S.D., and Davies, K.E. (2010). Prevention of dystrophic pathology in severely affected dystrophin/utrophin-deficient mice by morpholino-oligomer-mediated exon-skipping. Mol. Ther. *18*, 198–205.
31. Malerba, A., Sharp, P.S., Graham, I.R., Arechavala-Gomeza, V., Foster, K., Muntoni, F., Wells, D.J., and Dickson, G. (2011). Chronic systemic therapy with low-dose morpholino oligomers ameliorates the pathology and normalizes locomotor behavior in mdx mice. Mol. Ther. *19*, 345–354.
32. Betts, C.A., Saleh, A.F., Carr, C.A., Hammond, S.M., Coenen-Stass, A.M.L., Godfrey, C., McClorey, G., Varela, M.A., Roberts, T.C., Clarke, K., et al. (2015). Prevention of exercised induced cardiomyopathy following Pip-PMO treatment in dystrophic mdx mice. Sci. Rep. *5*, 8986.
33. Crisp, A., Yin, H., Goyenvalle, A., Betts, C., Moulton, H.M., Seow, Y., Babbs, A., Merritt, T., Saleh, A.F., Gait, M.J., et al. (2011). Diaphragm rescue alone prevents heart dysfunction in dystrophic mice. Hum. Mol. Genet. *20*, 413–421.
34. Fletcher, S., Honeyman, K., Fall, A.M., Harding, P.L., Johnsen, R.D., Steinhaus, J.P., Moulton, H.M., Iversen, P.L., and Wilton, S.D. (2007). Morpholino oligomer-mediated exon skipping averts the onset of dystrophic pathology in the mdx mouse. Mol. Ther. *15*, 1587–1592.
35. Rosenberg, A.S., Puig, M., Nagaraju, K., Hoffman, E.P., Villalta, S.A., Rao, V.A., Wakefield, L.M., and Woodcock, J. (2015). Immune-mediated pathology in Duchenne muscular dystrophy. Sci. Transl. Med. *7*, 299rv4.
36. Duddy, W., Duguez, S., Johnston, H., Cohen, T.V., Phadke, A., Gordish-Dressman, H., Nagaraju, K., Gnocchi, V., Low, S., and Partridge, T. (2015). Muscular dystrophy in the mdx mouse is a severe myopathy compounded by hypotrophy, hypertrophy and hyperplasia. Skelet. Muscle *5*, 16.
37. Battistoni, A., Rubattu, S., and Volpe, M. (2012). Circulating biomarkers with preventive, diagnostic and prognostic implications in cardiovascular diseases. Int. J. Cardiol. *157*, 160–168.
38. Sergeeva, I.A., Hooijkaas, I.B., Van Der Made, I., Jong, W.M.C., Creemers, E.E., and Christoffels, V.M. (2014). A transgenic mouse model for the simultaneous monitoring of ANF and BNP gene activity during heart development and disease. Cardiovasc. Res. *101*, 78–86.
39. Reiser, P.J., Portman, M.A., Ning, X.H., and Schomisch Moravec, C. (2001). Human cardiac myosin heavy chain isoforms in fetal and failing adult atria and ventricles. Am. J. Physiol. Heart Circ. Physiol. *280*, H1814–H1820.

40. Segawa, K., Komaki, H., Mori-Yoshimura, M., Oya, Y., Kimura, K., Tachimori, H., Kato, N., Sasaki, M., and Takahashi, Y. (2017). Cardiac conduction disturbances and aging in patients with Duchenne muscular dystrophy. Medicine (Baltimore) *96*, e8335.

41. Gonzalez, J.P., Ramachandran, J., Xie, L.-H., Contreras, J.E., and Fraidenraich, D. (2015). Selective Connexin43 Inhibition Prevents Isoproterenol-Induced Arrhythmias and Lethality in Muscular Dystrophy Mice. Sci. Rep. *5*, 13490.

42. Ishizaki, M., Maeda, Y., Kawano, R., Suga, T., Uchida, Y., Uchino, K., Yamashita, S., Kimura, E., and Uchino, M. (2011). Rescue from respiratory dysfunction by transduction of full-length dystrophin to diaphragm via the peritoneal cavity in utrophin/dystrophin double knockout mice. Mol. Ther. *19*, 1230–1235.

43. Gentil, C., Le Guiner, C., Falcone, S., Hogrel, J.-Y., Peccate, C., Lorain, S., Benkhelifa-Ziyyat, S., Guigand, L., Montus, M., Servais, L., et al. (2016). Dystrophin Threshold Level Necessary for Normalization of Neuronal Nitric Oxide Synthase, Inducible Nitric Oxide Synthase, and Ryanodine Receptor-Calcium Release Channel Type 1 Nitrosylation in Golden Retriever Muscular Dystrophy Dystrophinopathy. Hum. Gene Ther. *27*, 712–726.

44. Hösel, M., Huber, A., Bohlen, S., Lucifora, J., Ronzitti, G., Puzzo, F., Boisgerault, F., Hacker, U.T., Kwanten, W.J., Klöting, N., et al. (2017). Autophagy determines efficiency of liver-directed gene therapy with adeno-associated viral vectors. Hepatology *66*, 252–265.

45. Long, C., Amoasii, L., Mireault, A.A., McAnally, J.R., Li, H., Sanchez-Ortiz, E., Bhattacharyya, S., Shelton, J.M., Bassel-Duby, R., and Olson, E.N. (2016). Postnatal genome editing partially restores dystrophin expression in a mouse model of muscular dystrophy. Science *351*, 400–403.

46. van Westering, T.L.E., Lomonosova, Y., Coenen-Stass, A.M.L., Betts, C.A., Bhomra, A., Hulsker, M., Clark, L.E., McClorey, G., Aartsma-Rus, A., van Putten, M., et al. (2019). Uniform sarcolemmal dystrophin expression is required to prevent extracellular microRNA release and improve dystrophic pathology. J. Cachexia Sarcopenia Muscle. https://doi.org/10.1002/jcsm.12506.

47. Roy, P., Rau, F., Ochala, J., Messéant, J., Fraysse, B., Lainé, J., Agbulut, O., Butler-Browne, G., Furling, D., and Ferry, A. (2016). Dystrophin restoration therapy improves both the reduced excitability and the force drop induced by lengthening contractions in dystrophic mdx skeletal muscle. Skelet. Muscle *6*, 23.